de Azevedo-Quintanilha *et al. Malar J (2016) 15:393*
DOI 10.1186/s12936-016-1447-7

Malaria Journal

RESEARCH

Open Access

Integrin $\alpha_D\beta_2$ (CD11d/CD18) mediates experimental malaria-associated acute respiratory distress syndrome (MA-ARDS)

Isaclaudia G. de Azevedo-Quintanilha[1*†], Adriana Vieira-de-Abreu[2*†], André Costa Ferreira[1], Daniele O. Nascimento[1], Alessandra M. Siqueira[1], Robert A. Campbell[2], Tatiana P. Teixeira Ferreira[3], Tatiana M. Gutierrez[1], Gabriel M. Ribeiro[4], Patricia M. R. e Silva[3], Alysson R. Carvalho[5], Patricia T. Bozza[1], Guy A. Zimmerman[2] and Hugo C. Castro-Faria-Neto[1,6]

Abstract

Background: Malaria-associated acute respiratory distress syndrome (MA-ARDS) is a potentially lethal complication of clinical malaria. Acute lung injury in MA-ARDS shares features with ARDS triggered by other causes, including alveolar inflammation and increased alveolar-capillary permeability, leading to leak of protein-rich pulmonary oedema fluid. Mechanisms and physiologic alterations in MA-ARDS can be examined in murine models of this syndrome. Integrin $\alpha_D\beta_2$ is a member of the leukocyte, or β_2 (CD18), sub-family of integrins, and emerging observations indicate that it has important activities in leukocyte adhesion, accumulation and signalling. The goal was to perform analysis of the lungs of mice wild type C57Bl/6 ($a_D^{+/+}$) and Knockout C57Bl/6 ($a_D^{-/-}$) with malaria-associated acute lung injury to better determine the relevancy of the murine models and investigate the mechanism of disease.

Methods: C57BL/6 wild type ($a_D^{+/+}$) and deficient for CD11d sub-unit ($a_D^{-/-}$) mice were monitored after infection with 10^5 *Plasmodium berghei* ANKA. CD11d subunit expression RNA was measured by real-time polymerase chain reaction, vascular barrier integrity by Evans blue dye (EBD) exclusion and cytokines by ELISA. Protein and leukocytes were measured in bronchoalveolar lavage fluid (BALF) samples. Tissue cellularity was measured by the point-counting technique, F4/80 and VCAM-1 expression by immunohistochemistry. Respiratory function was analysed by non-invasive BUXCO and mechanical ventilation.

Results: Alveolar inflammation, vascular and interstitial accumulation of monocytes and macrophages, and disrupted alveolar-capillary barrier function with exudation of protein-rich pulmonary oedema fluid were present in *P. berghei*-infected wild type mice and were improved in $\alpha_D\beta_2$-deficient animals. Key pro-inflammatory cytokines were also decreased in lung tissue from $\alpha_D^{-/-}$ mice, providing a mechanistic explanation for reduced alveolar-capillary inflammation and leak.

Conclusions: The results indicate that $\alpha_D\beta_2$ is an important inflammatory effector molecule in *P. berghei*-induced MA-ARDS, and that leukocyte integrins regulate critical inflammatory and pathophysiologic events in this model of

*Correspondence: igomesdeazevedo@gmail.com; adrianav@u2m2.utah.edu
†Isaclaudia G. de Azevedo-Quintanilha and Adriana Vieira-de-Abreu contributed equally to this work
[1] Laboratório de Immunofarmacologia, Instituto Oswaldo Cruz, Fiocruz, Pavilhão Ozório de Almeida, Av. Brasil 4365, Manguinhos, Rio de Janeiro, RJ CEP 21045-900, Brazil
[2] Program in Molecular Medicine, Department of Internal Medicine, University of Utah, Salt Lake City, UT, USA
Full list of author information is available at the end of the article

complicated malaria. Genetic deletion of integrin subunit α_D in mice, leading to deficiency of integrin $\alpha_D\beta_2$, alters lung inflammation and acute lung injury in a mouse model of MA-ARDS caused by *P. berghei*.

Keywords: Integrin $\alpha_D\beta_2$, Acute lung injury, Acute respiratory distress syndrome, Inflammation, Malaria

Background

Malaria is an infectious disease that is caused by the genus *Plasmodium* sp. transmitted through the bite of Anopheles mosquitoes that are infected with protozoan parasites and is a major public health problem 40 % or more of the global population is at risk for malaria [1]. The pathogenesis of malaria is multi-factorial, with both host and *Plasmodium* sp. factors playing critical roles [2, 3]. Nevertheless, the mechanisms responsible for the high morbidity and mortality of severe cases of malaria remain poorly understood. In endemic areas, many infections in semi-immune population present as an uncomplicated febrile illness. In more severe cases, non-immune individuals may exhibit a number of syndromes including severe anaemia (SA), cerebral malaria (CM) or respiratory distress syndrome [4, 5].

Lung involvement in malaria has been described most often in non-immune individuals, with infection by *Plasmodium falciparum* [6–9], *Plasmodium ovale* [7, 10, 11], *Plasmodium vivax* and *Plasmodium malariae* [6, 7, 12–16]. While the alveoli and airways can also be involved in mild infection [17], acute alveolar injury and acute respiratory distress syndrome (ARDS) are major sequelae of severe malaria and have significant morbidity and mortality [3, 17–19]. Malaria-associated ARDS (MA-ARDS) has been reported in infection with all human malarial parasites, although the greatest number of cases is caused by *P. falciparum* and *P. vivax* [17, 20, 21]. Patients with alveolar involvement in malaria have classically been reported to have pulmonary oedema, with recent recognition that the alveolar oedema is due to increased pulmonary capillary permeability [21–24]. In addition to altered alveolar-capillary barrier function with leak of protein-rich oedema fluid [3, 22–24], which is a cardinal manifestation of acute alveolar inflammation, alveolar involvement in human malaria has other significant inflammatory components, including leukocyte accumulation [17, 21, 25–29]. Alveolar inflammation is also a fundamental feature of ARDS induced by bacterial sepsis, infectious pneumonia, aspiration of gastric contents, major trauma, and other common 'triggers' [30]. A difference is that, in these more common etiologies of ARDS, alveolar injury is thought to be primarily caused by neutrophil- and platelet-dependent damage to endothelial and epithelial barriers of the alveolar-capillary membrane [30, 31], whereas in MA-ARDS monocytes and macrophages dominate in the inflammatory infiltrate [21, 25–29]. MA-ARDS has been modelled in studies utilizing mice and other animals, yielding mechanistic insights and experimental correlates [21, 32–37]. There is evidence that lung injury in the murine model *Plasmodium berghei* ANKA strain [33, 34, 37, 38] is associated with intravascular sequestration of parasitized red blood cells [33, 39], suggesting that it is a useful surrogate for human malarial disease [26, 40].

Integrins are cell surface heterodimers formed by non-covalent association of α and β polypeptide chains (subunits). Integrins are widely expressed on mammalian cells and have multiple activities in cellular adhesion, migration, signalling, and fate [41, 42]. A sub-family of integrins, termed the β_2, CD18, or leukocyte integrins, share a common β_2 sub-unit and are expressed on circulating and tissue leukocytes [43, 44]. Four α chains pair with the β_2 peptide sub-unit to yield four leukocyte-restricted integrins: $\alpha_L\beta_2$ (CD11a/CD18, LFA-1), $\alpha_M\beta_2$ (CD11b/CD18, MAC-1, CR3), $\alpha_X\beta_2$ (CD11c/CD18), and $\alpha_D\beta_2$ (CD11d/CD18) [43, 44]. Leukocyte β_2 integrins are required for host defence against many pathogens and for tissue surveillance and repair, as demonstrated by deficiency syndromes that cause recurrent infections and impaired wound healing in humans and animals [44, 45]. In contrast, however, β_2 integrin-mediated activities of leukocytes also contribute to tissue injury in a variety of inflammatory syndromes [46].

Integrin $\alpha_D\beta_2$, the most recently identified β_2 integrin, is expressed on human and murine leukocytes, although its basal expression is different in man and mouse [47–51]. Integrin $\alpha_D\beta_2$ is expressed on tissue leukocytes in human inflammatory syndromes, including atherosclerosis [48], arthritis [52], and ARDS [51]. In rodents, there is evidence that $\alpha_D\beta_2$ can be induced on macrophages or monocytes in the spleen and liver [50], lung [53], and blood [54] in response to inflammatory challenge, and that $\alpha_D\beta_2$ contributes to inflammatory tissue damage in experimental spinal cord and brain injury [55–57]. Previously, Miyazaki et al. [50] found that genetic deletion of α_D in mice, leading to deficiency of $\alpha_D\beta_2$, alters survival and systemic cytokine levels in mice infected with *P. berghei* without altering parasitaemia or anaemia. $\alpha_D\beta_2$ influences the pathogenesis of experimental cerebral malaria in *P. berghei* infection (unpublished studies). In this work was examined $\alpha_D\beta_2$ in lung involvement in *P. berghei* -infected animals and found that it influences key features of acute lung injury in this model of experimental MA-ARDS.

Methods

Mouse models of malaria

The Animal Welfare Committee of the Oswaldo Cruz Institute approved the experiments in these studies under the licence number L-033/09. Wild Type ($a_D^{+/+}$) and C57BL/6 deficient for CD11d integrin ($a_D^{-/-}$) mice [50] weighing 20–25 g were obtained from the Oswaldo Cruz Foundation breeding unit and used throughout the study. The animals were kept at constant temperature (25 °C) with free access to food and water in a room with a 12-h light/dark cycle. C57BL/6 mice were infected by an ip injection of 200 mL of PBS containing 10^5 red blood cell (RBC) parasitized with the Pasteur strain of *P. berghei* ANKA [58]. All analyses were performed at day 7 post-infection. Between 90 and 100 % of infected mice developed lung injury and cerebral malaria (data about cerebral malaria not yet published).

Bronchoalveolar lavage fluid analysis

Infected and uninfected mice were euthanized using isoflurane (Abott Labs do Brasil LTDA) and bronchoalveolar lavage fluid (BALF) from both lungs was performed by instillation and aspiration of 1 mL of cold 1× phosphate buffered saline (PBS) [33]. Total leukocytes (diluted in Turk's 2 % acetic acid fluid) were counted using Neubauer chamber hemocytometer. Differential counts were performed in cytospins (Cytospin3, Shandon, CA, USA) and stained by the May-Grünwald-Giemsa method. The BALF was spun at 350 g at room temperature for 5 min, and the supernatant was removed and stored at −80 °C for further analyses. BALF total protein concentration was measured using a BCA protein assay kit (Thermo Scientific, Waltham, MA, USA).

Lung permeability

Mice were injected intravenously (iv) with 0.2 mL of 2 % Evans Blue dye (Sigma-Aldrich Brasil LTDA, São Paulo, Brazil) and were sacrificed 1 h later. Before collecting lung, mice were perfused with PBS 1X. The lungs were collected and placed in 2 mL of formamide (VETEC Química Fina LTDA, Duque de Caxias, RJ, Brazil) at 37 °C, overnight to extract Evans Blue dye from the tissue [59]. Absorbance was measured at $\lambda = 620$ nm (Molecular Devices Spectra Max 190, Sunnyvalle, CA, USA). Evans Blue dye concentration was calculated from a standard curve and is expressed as mg of Evans Blue dye per lung tissue.

Lung histology

Before collecting lung, mice were perfused with PBS 1X. Lungs from infected and uninfected mice were inflated by injecting 1.0 mL of 10 % buffered formalin through the same catheter used to perform BALF. Lungs were removed fixed in formalin and embedded in paraffin. Lungs sections of 5-mm thickness were stained with haematoxylin-eosin [59]. Analysis of tissue sections was performed in a Olympus BX41 microscope (Melville, NY, USA) at a magnification of ×200. The number of mononuclear cells in lung tissue was determined by the point-counting technique across 20 random, non-coincidents microscopic fields in an Olympus BX41 microscope at a magnification of ×1000 [60].

Cytokine determinations

Before collecting lung, mice were perfused with PBS 1X. Lungs of infected and uninfected mice were excised and homogenized in 750 mL of a protease inhibitor cocktail (Complete, mini EDTA-free Roche Applied Science, Mannheim, Germany) for 30 s, using a Ultra-Turrax Disperser T-10 basic (IKA-Guangzhou, China). Homogenates were stored at −20 °C, for analysis of cytokines using a commercial ELISA kit according to the manufacturer's instructions (R&D Systems Duo set kits, Minneapolis, USA).

Quantitative RT-PCR

Before collecting lung and spleen, mice were perfused with PBS 1X. Extraction of total RNA from lungs and spleen was performed using TRIzol® (Invitrogen, Carlsbad, CA, USA), according to the manufacturer's instructions. After extraction, RNA concentration and quality were determined using a NanoDrop 2000 spectrophotometer (Thermo Scientific). One microgram of total RNA was reverse-transcribed to single-strand cDNA using the SuperScript First-Stand (Invitrogen). a_D transcripts in the cDNA pool obtained from the reverse transcriptase reaction were quantified by real-time quantitative fluorogenic PCR. TaqMan Universal PCR Master Mix (Applied Biosystems, Foster City, CA, USA) was used to quantify gene expression according to the manufacturer's instructions. RNA expression levels were calculated using the Data Assist Software v.3, and normalized against the expression levels of the housekeeping gene hypoxanthine guanine phosphoribosyl transferase (HPRT) [50]. The primers used were as follows: a_D (TaqMan-murine-Mm01159115_m1) and HPRT (TaqMan-murine- Mm01545399_m1).

Immunofluorescence

The primary monoclonal antibodies used in immunofluorescence reactions were VCAM-I (rat anti-Mouse CD106, eBioscience, San Diego, CA, USA) and negative control (rat anti-IgG2b, Bioscience). Before collecting lung, mice were perfused with PBS 1X. Lung tissues from infected and uninfected mice $a_D^{+/+}$ and $a_D^{-/-}$ were frozen in tissue freezing medium (TBS™, Triangle Biomedical

Science, Inc, Durham, NC, USA) and 10-mm cryostat sections were deposited on 3-aminopropyl triethoxysilane (Sigma-Aldrich) prepared slides. The sections were then fixed in 2 % paraformaldehyde and permeabilized with 0.01 % Triton X-100 (Sigma) for 10 min. Sections were then blocked with 10 % normal goat serum, for 40 min and subsequently incubated with primary antibody overnight at 4 °C. Alexa 546-conjugated goat anti-rat antibody was applied 1/1000 dilution and incubated for 40 min. The sections were then layered with anti-fade medium conjugated with DAPI (Vectashield, Vector Laboratories, Burlingame, CA, USA). The slides were analysed by confocal laser scanning microscopy on Zeiss LSM 510-META (Jena, Germany).

Immunohistochemistry

Primary monoclonal antibodies used in immunohistochemistry reactions were F4/80 (MCA497-Serote c; anti-rat) and IgG-HRP (STAR72-Serotec; goat anti rat) were also used in immunohistochemistry reactions. After deparaffinization, the sections were hydrated with TBS (Tris/HCl 0.05 M + NaCl 0.5 M, pH 7.6), and H_2O_2 in methanol 3 % was add for 15 min. Slides were washed with TBS and blocked with Tris–HCl + BSA 5 % for 2 h and subsequently incubated with primary antibody diluted Tris–HCl + BSA 1 % for 12 h at 4 °C. After incubation, the slides were washed with TBS. The secondary antibody HRP-conjugated was diluted in Tris–HCl and incubated for 2 h. The revealed was made with 3-amino-9-ethylcarbazole (AEC) for 15 min. The slides were washed with distilled water, counterstained with haematoxylin of Mayer and mounted in an aqueous medium-containing gelatin. The slides were analysed using a Olympus BX41 microscope at a magnification of ×200.

Airway hyperreactivity analysis

Airway hyperreactivity (AHR) [61] was analysed in infected and uninfected mice using non-invasive whole-body plethysmography (Buxco, Sharon, Connecticut, CT, USA) 7 days' post infection. AHR was measured after aerosolization of 1× PBS followed by increasing concentrations of methacholine (0, 171, 6, 25 mg/mL; Sigma-Aldrich) for 7 min into the chamber. AHR was expressed as an average enhanced pause [38]. There was an interval of 10 min between each aerosol exposure and within this period of time the Penh values had returned to baseline.

Lung pressure/volume analysis in mechanically ventilated mice

Pressure/volume (PV) relationships was examined in mechanically ventilated wild type and $\alpha_D^{-/-}$ uninfected and PbA-infected in mice. After 40 s of stabilization period under baseline settings (V_T of 8–10 mL/kg, RR of 80 breaths/min, ratio I:E of 1:1 and PEEP of 2 cm H_2O), RR was decreased to 6 breaths/min, PEEP of 0 cmH_2O, I:E ratio set at 4:1, V_T was increased to 25–30 mL/kg and three PV curves were obtained. Airway pressure was continuously measured with a differential pressure transducer (UT-PDP-50, SCIREQ, Canada) at the distal end of the endotracheal tube (ETT). Airflow was measured with a heated-controlled pneumotachograph connected to a pressure transducer and positioned between the ETT and the Y-piece of the mechanical ventilator. Paw and airflow signals were low-pass filtered at 30 Hz, digitized at 1000 Hz and recorded with a purpose-built software (Data Acquisition System) written in LabVIEW® (National Instruments, Austin, TX, USA). Volume was then calculated by numerical integration of airflow. The PV curves where peak airway pressure remains stable and near to 20 cm H_2O were fitted with a sigmoidal model (Eq. 1):

$$V = a + \left[b \Big/ \left(1 + e^{(- Pel(V) - c/d)} \right) \right] \quad (1)$$

where Pel is the elastic pressure, V is the Volume, and a, b, c and d are the coefficients of the model, obtained by nonlinear fitting with the Levenberg–Marquardt method. The point of maximal compliance (PMC) is equivalent to the parameter c of this model and was estimated for each animal.

Statistical analysis

Statistical analysis was carried out using the GraphPad Prism software (San Diego, CA, USA). P values were calculated by unpaired Student's t test, except for PMC calculated with Wilcoxon rank sum test. Results are expressed as mean ± SEM (median (IQR)). The level of significance was set at $P \leq 0.05$.

Results

Expression of α_D mRNA transcripts is increased in the lung in *Plasmodium berghei* infection

Transcripts for α_D in the lungs of wild type mice were examined in the basal state and after infection with *P. berghei*. RT-PCR analysis of mRNA extracted from lungs of naïve, uninfected animals demonstrated a low level of the α_D transcript. The expression of α_D increased dramatically at 7 and 10 days after infection with *P. berghei* and approached levels detected in the spleen (Fig. 1), where $\alpha_D\beta_2$ integrin is constitutively expressed [50].

Disrupted alveolar-capillary membrane barrier function and alveolar inflammation are ameliorated in $\alpha_D\beta_2$-deficient mice

Infection with *P. berghei*, induces alveolar-capillary barrier disruption and lung edema in mice of several backgrounds [33–37]. Consistent with these observations

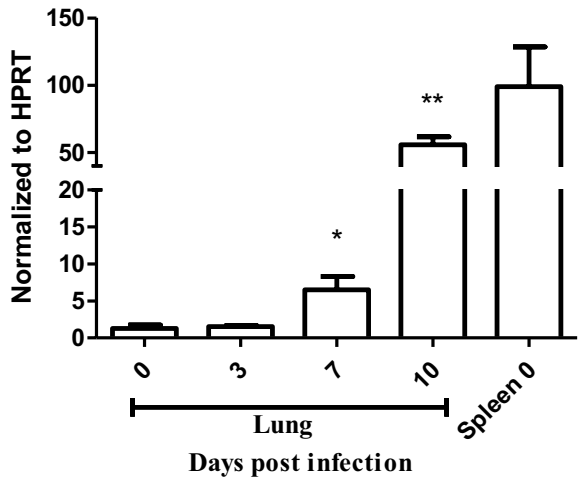

Fig. 1 α_D mRNA expression is increased in the lungs of mice infected with *Plasmodium berghei* ANKA. Infected wild type were sacrificed 7 or 10 days later. Lungs were removed, processed and reverse transcribed. Transcripts for α_D were quantified by real-time quantitative PCR and normalized to the levels of hypoxanthine guanine phosphoribosyl transferase (*HRPT*). Expression of α_D in spleen was used as a positive control. Each *bar* represents the mean ± SEM of determinations in tissue from 5 animals. *P ≤ 0.04, **P ≤ 0.001 by student's t test

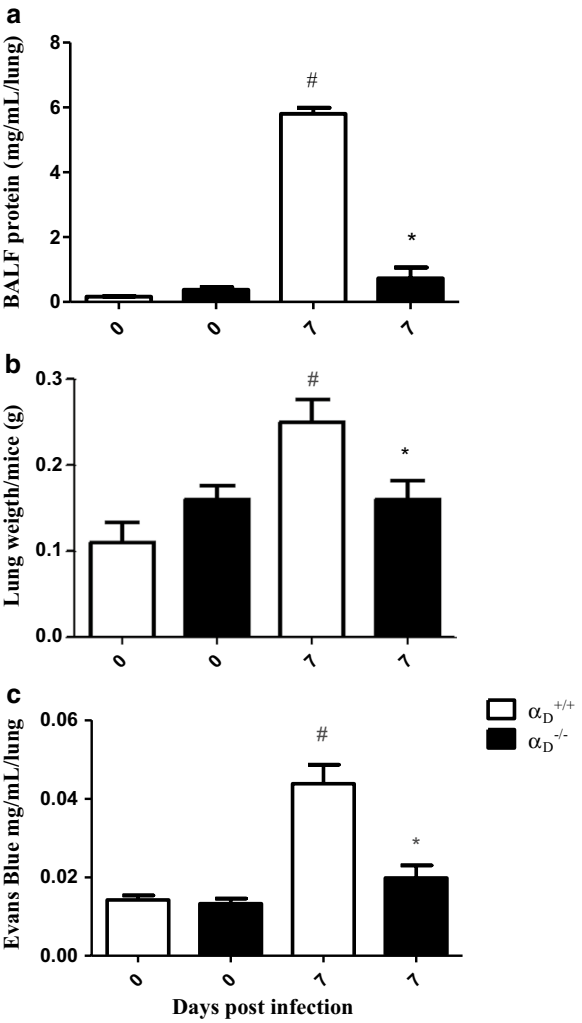

Fig. 2 Alveolar-capillary barrier disruption and increased permeability pulmonary are ameliorated in $\alpha_D\beta_2$-deficient mice infected with *Plasmodium berghei* ANKA. Infected wild type ($\alpha_D^{+/+}$) and $\alpha_D\beta_2$-deficient ($\alpha_D^{-/-}$) were study 7 days after infection. Bronchoalveolar lavage fluid (BALF) was performed. **a** Total protein concentration was measured in BALF samples using a BCA protein determination assay. **b** A second group of animals was sacrificed without BALF and the lungs were removed and weighed immediately after sacrifice. **c** In a third group of $\alpha_D^{+/+}$ and $\alpha_D^{-/-}$ mice, Evans Blue Dye (2 %, 0.2 mL) was injected intravenously. The animals were sacrificed 1 h later, and Evans Blue Dye concentration in the lung tissue. Each *bar* in panels **a**–**c** indicates the mean ± SEM. of determinations from 5 animals.$^{\#}$P ≤ 0.05 compared to the respective control group; P ≤ 0.05 compared to $\alpha_D^{+/+}$ infected mice

protein concentration in BALF samples (Fig. 2a), lung weight (Fig. 2b), and lung endothelial permeability as measured by extravasation of Evans Blue dye (Fig. 2c) were increased in wild type mice infected with *P. berghei*. Similar alterations in these variables are seen in murine acute lung injury induced by other insults [62] and are key correlates of disrupted alveolar-capillary barrier integrity and increased permeability pulmonary oedema, which are cardinal features of clinical and experimental ARDS [30, 31, 62]. Each variable was improved to near basal levels in $\alpha_D^{-/-}$ mice infected with *P. berghei* compared to measurements in infected wild type animals (Fig. 2a–c), indicating that alveolar-capillary barrier disruption is ameliorated in mice deficient in $\alpha_D\beta_2$. Focal haemorrhages, which were scattered throughout the inflamed lung parenchyma of P. *berghei*-infected wild type mice (Fig. 3), were less frequent in $\alpha_D\beta_2$-deficient mice. The latter finding is also consistent with amelioration of endothelial leakiness in $\alpha_D^{-/-}$ animals.

Accumulation of leukocytes was found in the lungs of wild type mice infected with *P. berghei* (Fig. 3). Nevertheless, increased leukocyte numbers was not detected in the alveolar spaces as demonstrated by cell counts in BALF samples (total BALF cell numbers in wild type *P. berghei*-infected mice $4.86 \times 10^5 \pm 0.7502$ cells/mL compared to $4.165 \times 10^5 \pm 0.4847$ cells/mL in uninfected wild type controls P = 0.4863). This finding, and microscopic analysis (Figs. 3, 4), indicated that the primary accumulation of leukocytes is in the alveolar vessels and interstitium rather than in the alveolar space under these conditions. This distribution of inflammatory cells in the lungs was also reported in previous studies of *P. berghei*-infected C57BL/6 mice [33]. To better characterize

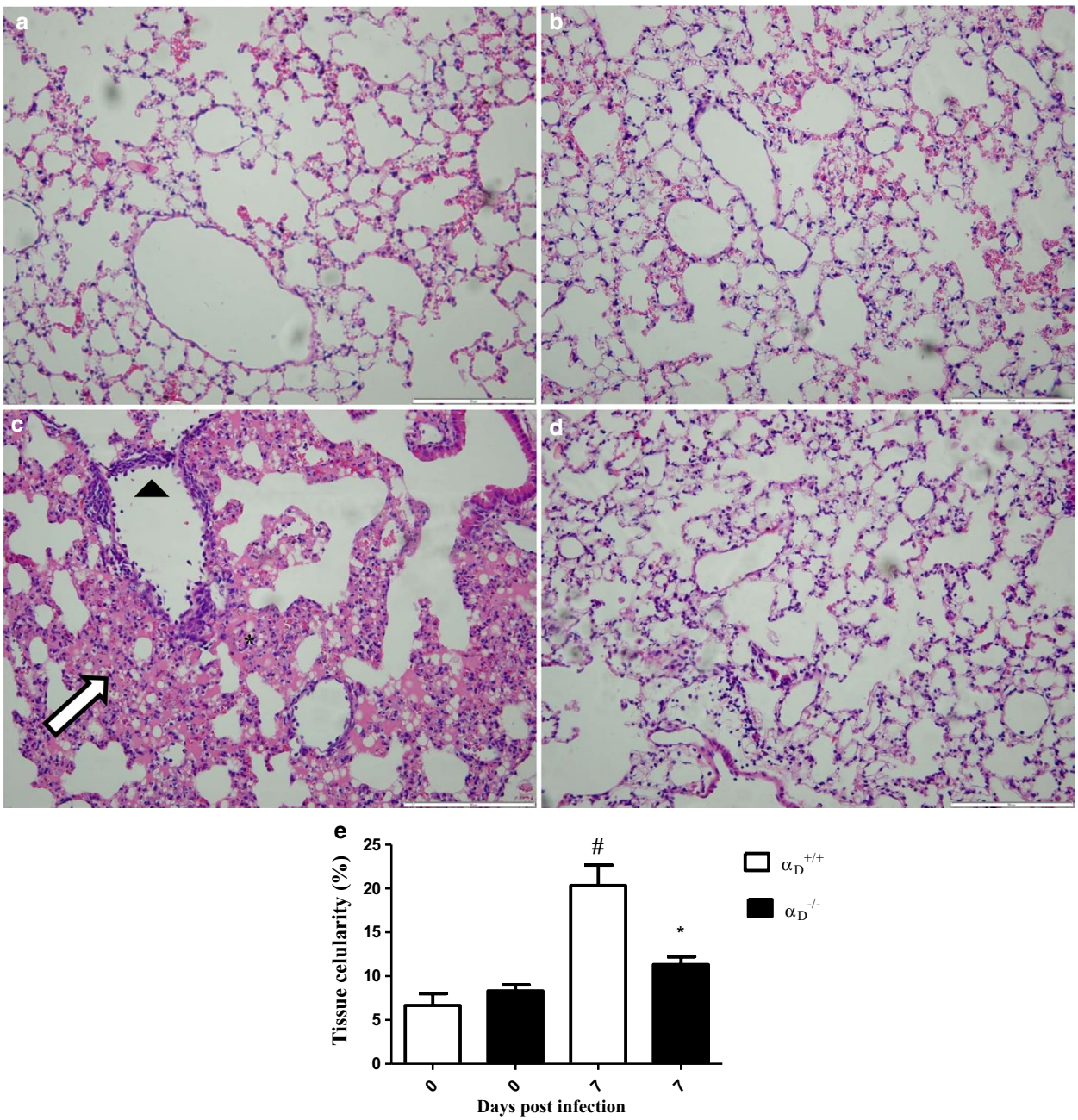

Fig. 3 Vascular and interstitial inflammation are key components of MA-ARDS in *Plasmodium berghei* ANKA-infected mice. After staining with haematoxylin-eosin, the sections were examined by optical microscopy (×200 magnification). The *scale bars* indicate 50 µm. **a** Lung tissue from an uninfected $\alpha_D^{+/+}$ mouse. **b** Lung section from an uninfected $\alpha_D^{-/-}$ animal. **c** Lung tissue from an infected wild type $\alpha_D^{+/+}$ animal. The *arrowhead* identifies adherent leukocytes in a pulmonary vessel, indicating vascular inflammation. Diffuse interstitial infiltrates (*arrow*) and focal haemorrhages (*asterisks*) were also seen. **d** Lung tissue section from an infected $\alpha_D^{-/-}$ mouse. The features illustrated in **a**–**d** are representative of those seen in lung tissue from 3 individual mice in each condition. **e** Lung cellularity was determined by the point counting technique across 20 random, non-coincident microscopic fields at magnification of ×1000, as described in "Methods" section. Each *bar* represents the mean of determinations in tissue from 3 animals ± SEM.$^{\#}P \leq 0.05$ compared to respective control

leukocytes that accumulated in the alveolar interstitium of mice infected with *P. berghei,* lung sections from infected animals were stained with mAb F4/80 and high frequency of positive cells was observed (Fig. 4). This indicates that macrophages and monocytes are the major leukocyte types accumulating in the lungs of *P. berghei*-infected

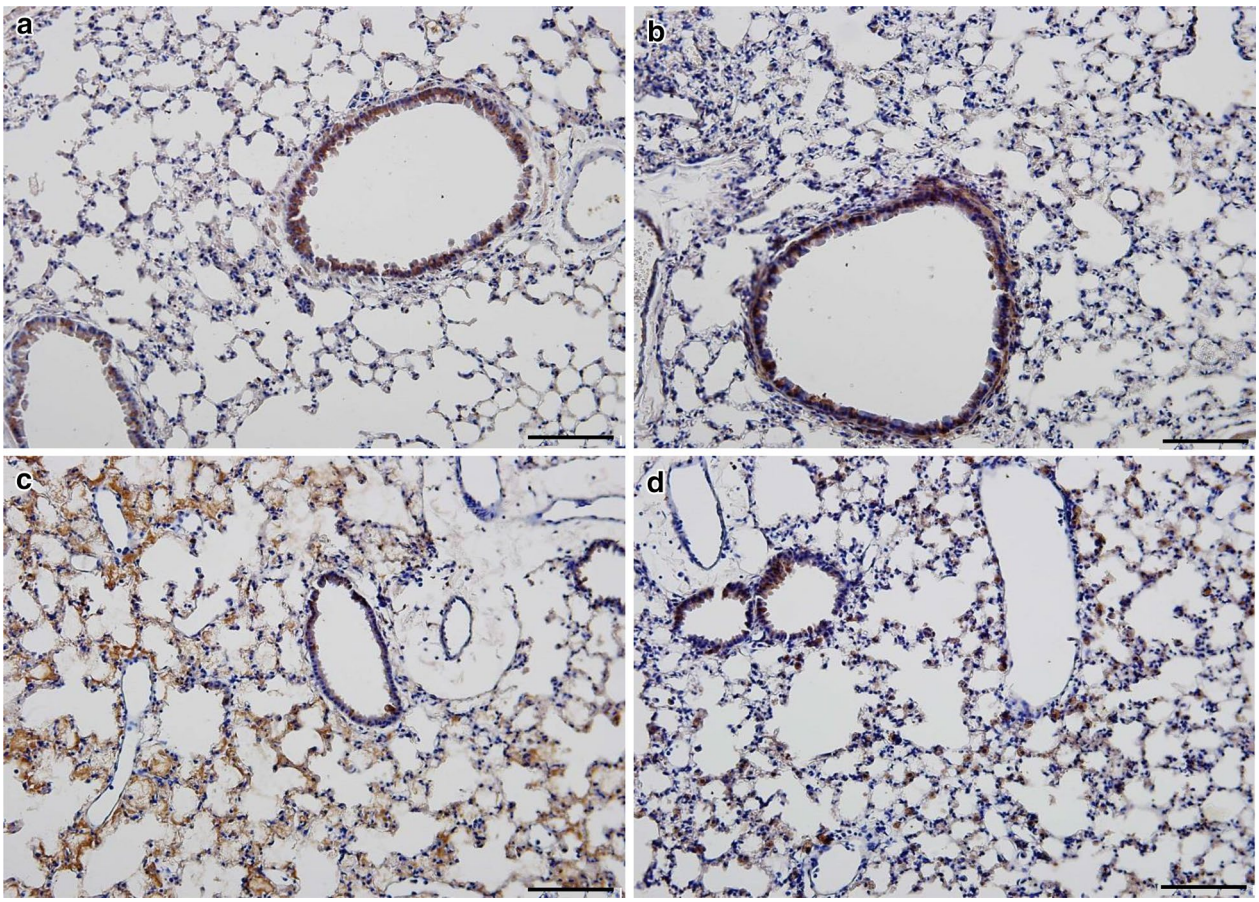

Fig. 4 F4/80-positive leukocytes accumulate in the alveoli in *Plasmodium berghei* ANKA-induced experimental MA-ARDS and are reduced in $\alpha_D\beta_2$-deficient mice. Lung tissue from $\alpha_D^{+/+}$ and $\alpha_D^{-/-}$ mice infected with *P. berghei* was harvested at 7 days after infection. Lung slices were incubated with anti-F4/80 as the primary antibody and HRP-conjugated secondary antibody. The sections were examined and photographed using an Olympus BX41 microscope at ×200 magnification (*scale bars* 200 mm). **a** Sections from a control $\alpha_D^{+/+}$ mouse. **b** Section from a control $\alpha_D^{-/-}$ mouse. **c** Lung tissue from an infected $\alpha_D^{+/+}$ wild type animal. **d** Section from an infected $\alpha_D^{-/-}$ mouse. The staining patterns shown in **a**–**d** are representative of those in lung tissue from 3 individual mice for each condition

animals at 7 days post-infection [63, 64]. In conclusion, the findings in this model are similar to descriptions of alveolar inflammation and accumulation of monocytes and macrophages in alveolar vessels and the interstitium in histopathologic specimens from the lungs of patients who died with MA-ARDS [3, 21, 25, 28, 29].

Lung cellularity and alveolar leukocyte accumulation were dramatically reduced in samples from $\alpha_D^{-/-}$ mice infected with *P. berghei* compared to leukocyte accumulation in lungs of infected wild type animals (Fig. 3). Consistent with this, the frequency of F4/80-positive leukocytes was reduced in $\alpha_D\beta_2$-deficient mice (Fig. 4). In addition, leukocytes adherent to the endothelium of pulmonary vessels were reduced in lung sections from infected $\alpha_D^{-/-}$ mice when compared to sections from infected wild type animals (Fig. 3).

To further characterize the decreased cellularity and leukocyte accumulation in the lungs of $\alpha_D^{-/-}$ mice, expression of VCAM-1, an important ligand for $\alpha_D\beta_2$ [50, 65, 66] was examined. Increased expression of VCAM-1 was observed in the lungs of infected animals. Increased VCAM-1 staining was similar in the $\alpha_D^{+/+}$ and $\alpha_D^{-/-}$ genotypes (Fig. 5), indicating that expression of this adhesive ligand is not altered by the genetic manipulation and suggesting that the decrease in leukocyte accumulation in the lungs of $\alpha_D^{-/-}$ animals (Figs. 3, 4) is due to deficiency of $\alpha_D\beta_2$.

Inflammatory cytokines are decreased in the lungs of $\alpha_D\beta_2$-deficient mice infected with *Plasmodium berghei*

To explore mechanisms related to decreased acute lung injury and inflammation in $\alpha_D\beta_2$-deficient mice with experimental MA-ARDS, inflammatory cytokines

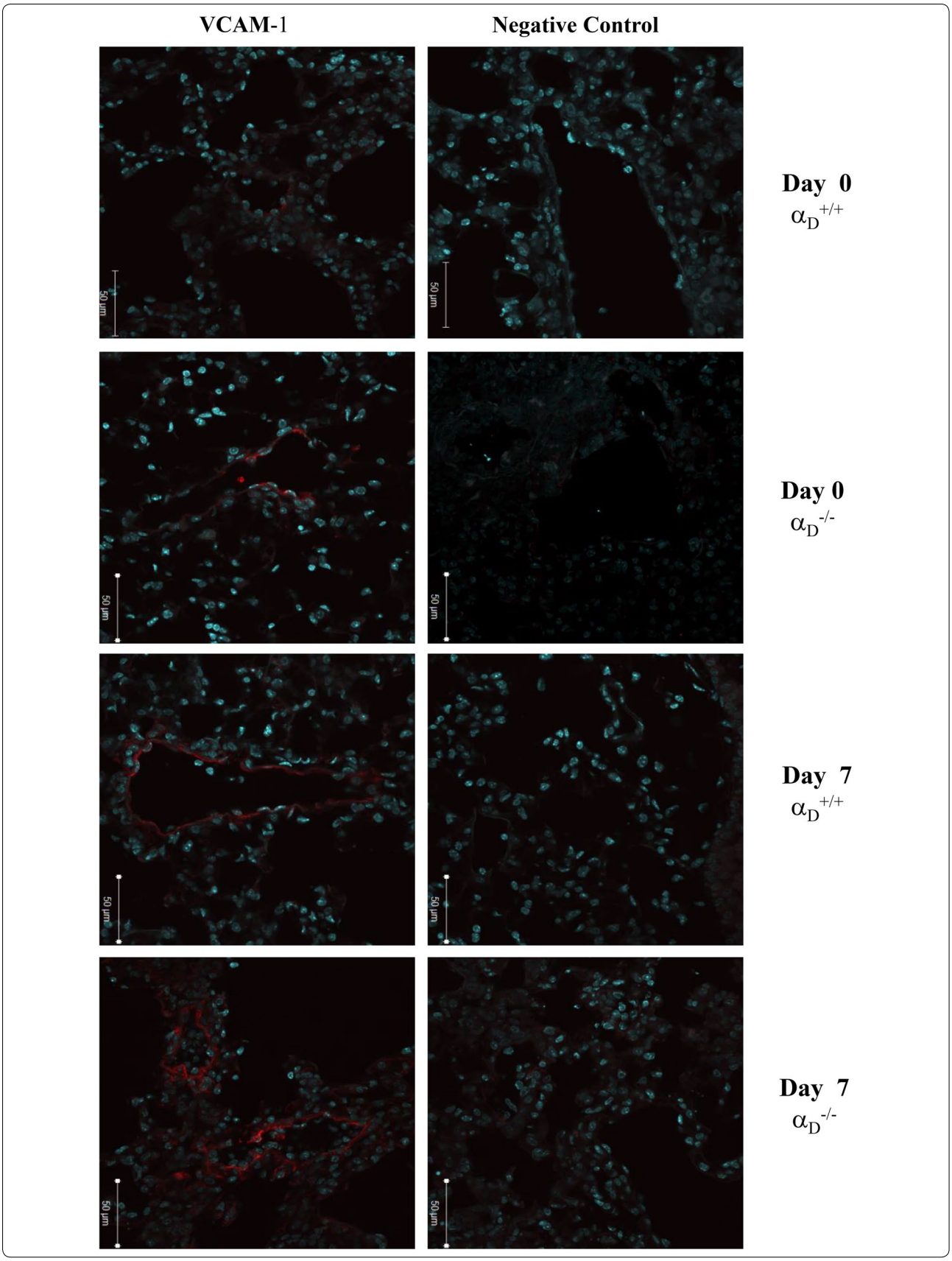
VCAM-1
Negative Control
Day 0
$\alpha_D^{+/+}$
Day 0
$\alpha_D^{-/-}$
Day 7
$\alpha_D^{+/+}$
Day 7
$\alpha_D^{-/-}$
50 µm

(See figure on previous page.)
Fig. 5 VCAM-1 expression is increased in the lungs of wild type and $\alpha_D\beta_2$-deficient mice after infection. Wild type and $\alpha_D\beta_2$-deficient mice were infected with PbA and lungs were harvested at sacrifice at 7 days of infection. Lungs from infected wild type animals at day 0 were also obtained and handled in the same fashion. Staining for VCAM-1 was accomplished with a specific fluorescently labelled rat anti-mouse antibody (red staining). A rat anti-mouse IgG2b was used as an irrelevant control antibody. Nuclei were stained with DAPI. The sections were examined and photographed by immunoflourescent microscopy at ×20 magnification (50 μm). The patterns shown in the panels are representative of those seen in samples from 3 individual animals for each condition

were measured in lung homogenates from $\alpha_D^{-/-}$ and wild type animals collected 7 days after *P. berghei* infection. Concentrations of tumour necrosis factor (TNF), interleukin-1β (IL-1β), interleukin 6 (IL-6), interleukin-12 (IL-12), monocyte chemotactic protein 1 (MCP-1), regulated upon activation normal T cell expressed and secreted (RANTES), and the murine orthologue of interleukin-8 (IL-8), KC, were increased in lungs of wild type $\alpha_D^{+/+}$ animals (Fig. 6). The level of each of these cytokines was lower in lung lysates from $\alpha_D\beta_2$-deficient mice, and in some cases was similar to that detected in samples from uninfected control animals (Fig. 6).

Airway hyper-responsiveness and obstruction are induced by *Plasmodium berghei* infection and are improved in *P. berghei*-infected mice deficient in $\alpha_D\beta_2$

Although alveolar-capillary membrane injury and MA-ARDS are the principal features of pulmonary involvement in malaria [21] some patients have evidence for airway dysfunction, including cough and airway obstruction documented by spirometry and pulmonary function assessment [6, 17]. *P. berghei*-infected mice showed increased airway reactivity that is further increased by methacholine challenge at 7 days post-infection (Fig. 7). The physiologic alterations in the basal state and the enhanced responses to methacholine indicate airway hyper-responsiveness [67] in wild type $\alpha_D^{+/+}$ animals infected with *P. berghei*. In infected $\alpha_D^{-/-}$ mice airway hyper-responsiveness was abrogated in both the basal state and after methacholine administration (Fig. 7).

Lung pressure/volume relationships are altered by *Plasmodium berghei* infection

All PV curves were sigmoidal and PMC values were lower in infected groups. The expected sigmoidal shape of the PV curves indicated a predominance of cyclic recruitment at the lower portion of the curve followed by a linear region and a predominance of hyperdistention in the upper portion (Fig. 8a). In infected mice of both genotypes, respiratory system compliance was decreased with lower volumes at equal pressures, with an increase in hyperdistention and a decrement of the PCM pressure (Fig. 8b). There was a trend toward improvement ($P = 0.064$) in the PMC values for infected $\alpha_D^{-/-}$ mice (Fig. 8b).

Discussion

Complicated malaria is a major challenge in management of malarial infections, which are dominant global public health problems [3]. Pulmonary complications are among the most serious and potentially lethal consequences of malaria [18, 19, 22], and it is clear that they occur in human malarial infections caused by parasite species in addition to *P. falciparum*, including *P. vivax* and *Plasmodium knowlesi* [17, 20, 21, 26, 28, 29]. MA-ARDS is the most fulminant syndrome of lung involvement in malaria [18, 19, 21] and, like ARDS induced by other infectious and non-infectious causes [30, 31, 68], is characterized by generation of pro-inflammatory cytokines, acute alveolar inflammation, disrupted alveolar capillary membrane barrier function, and increased permeability pulmonary oedema [19, 21]. Alveolar involvement in MA-ARDS may be due in part to organ-specific, local intravascular inflammation and unique events such as release of toxins from parasitized RBCs sequestered in the lung [37, 69, 70]. Mouse models have the potential to reveal key mechanistic features and common and divergent organ-specific responses in MA-ARDS, cerebral malaria, and other complicated malarial syndromes [21, 40, 69]. The present study provides additional evidence that acute alveolar injury in the *Plasmodium berghei* ANKA model of MA-ARDS has features similar to those in humans with clinical MA-ARDS [19, 21], including increased permeability pulmonary oedema, vascular and interstitial inflammation with accumulation of alveolar monocytes and macrophages, focal parenchymal haemorrhages, and pulmonary generation of cytokines. In addition, AHR and obstruction are elements of lung involvement in the *P. berghei* model, as they are in some patients with complicated and uncomplicated clinical malaria [6, 17, 19]. Moreover, *P. berghei* infection alters respiratory system elastic components, consistent with alveolar and airway inflammation. It is important to note that changes in PV relationships are late responses to progressive pulmonary involvement, and with a more extended time course this tends to worsen. Together, these measurements indicate that *P. berghei* infection induces substantial alterations in physiologic lung and airway function that accompanies lung inflammation and oedema. Finally, this model was used to examine regulation of key events in *P. berghei*-induced lung inflammation by an important leukocyte integrin, $\alpha_D\beta_2$.

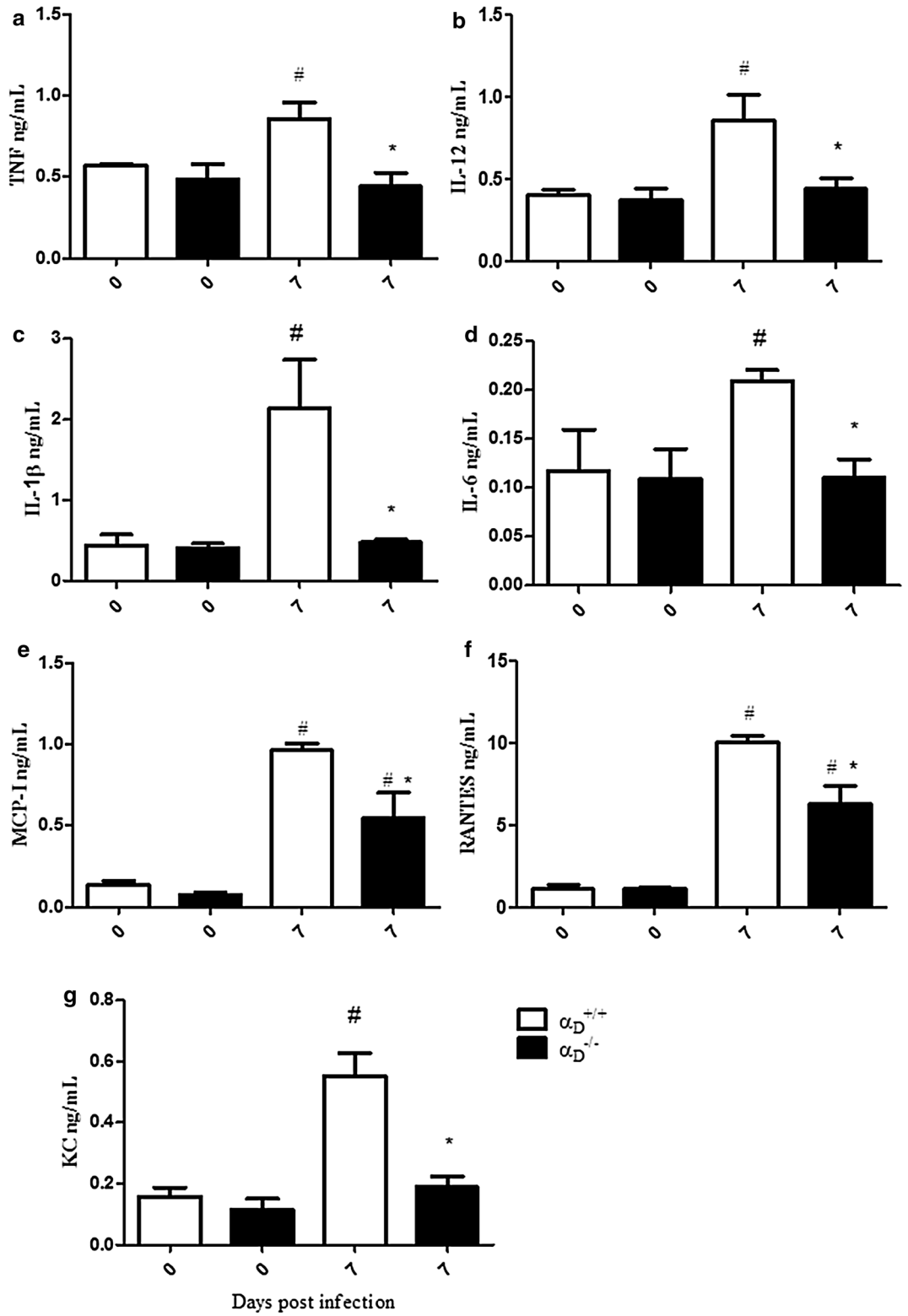

Fig. 6 Inflammatory cytokines are decreased in the lungs of $\alpha_D\beta_2$-deficient mice in *Plasmodium berghei* ANKA-induced MA-ARDS. Wild type and $\alpha_D\beta_2$-deficient mice were infected with PbA and lungs were harvested at 7 days after infection. Cytokine and chemokine levels were measured in the homogenates by ELISA. **a** TNF. **b** IL-12. **c** IL-1b. **d** IL-6. **e** MCP-I. **f** RANTES. **g** KC. Each *bar* indicates the mean ± SEM. of determinations in lung samples from 5 individual animals. $^{\#}P \leq 0.05$ compared to the respective control group; $^{*}P \leq 0.05$ compared to infected wild type ($\alpha_D^{+/+}$) mice

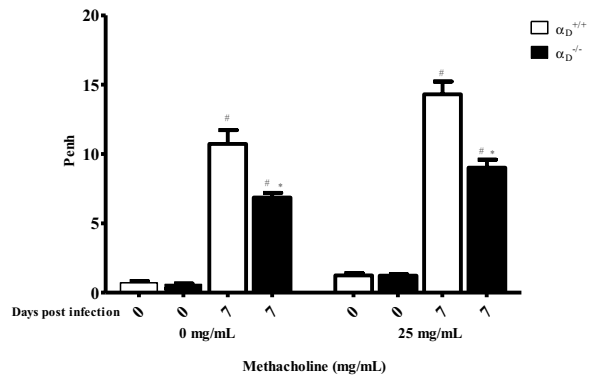

Fig. 7 *Plasmodium berghei* ANKA infection induces increased airway reactivity that is ameliorated in $\alpha_D\beta_2$-deficient mice. Infected $\alpha_D\beta_2$-deficient and wild type mice were studied 7 days after infection. Uninfected $\alpha_D^{-/-}$ and $\alpha_D^{+/+}$ animals were also studied as controls. Airway hyperreactivity was evaluated by challenge of the animals with aerosolized phosphate buffered saline (PBS) followed by methacholine (25 mg/mL in PBS) and is expressed as average enhanced pause (Penh). Each *bar* represents determinations in 10 animals (mean ± SEM). $^{\#}P \leq 0.05$ compared to the respective control group; $^{*}P \leq 0.05$ compared to infected $\alpha_D^{+/+}$ mice

β_2 integrins have critical activities in leukocyte biology, including regulation of adhesion, targeting and accumulation in infected or injured tissue sites, apoptosis, activation and inflammatory signalling, and immune interactions [42, 44, 45, 71]. Thus, β_2 integrins are members of a complex fabric of effector molecules that regulate leukocyte participation in infectious, inflammatory and immune host responses. Integrin $\alpha_D\beta_2$ is the most recently identified β_2 integrin [44, 48], and its specific contributions to infectious and inflammatory pathologies are largely unexplored. Experiments in this study indicate that it has major effector activities in experimental MA-ARDS induced by *P. berghei*. Expression of transcripts coding for the α_D subunit were increased in the lungs of mice infected with *P. berghei*. Increased α_D transcripts may have been due to accumulation of α_D-expressing monocytes or other α_D-expressing leukocytes from the blood [54], induction of α_D expression in resident alveolar macrophages and other lung myeloid leukocytes [50, 53], or both mechanisms. While this issue remains to be resolved, increased expression of α_D in the

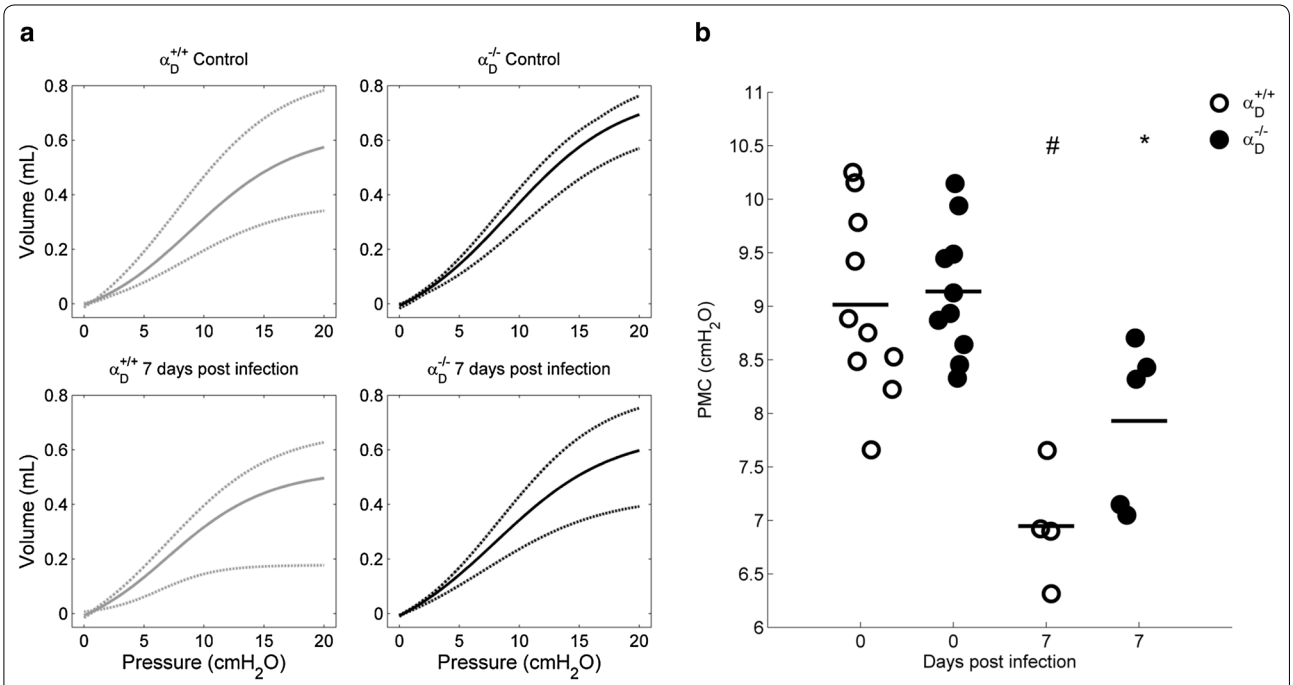

Fig. 8 Pressure/volume curves are sigmoidal and PMC is decreased in *Plasmodium berghei* ANKA-infected mice. Wild type and $\alpha_D^{-/-}$animals from infected and control groups were mechanically ventilated and three PV curves were obtained (RR = 6 breaths/min, PEEP = 0 cm H_2O, I:E ratio = 4:1, V_T = 25–30 mL/kg). The PV curves where peak airway pressure remains stable and near to 20 cm H_2O were fitted according to Eq. 1. The curve model gives the pressure value at which the respiratory system has maximum compliance. **a** *Upper* (*dashdot*), mean (*solid*) and *lower* (*dashed*) fitted curves of each group. **b** The PMC are lower, for infected wild type ($P < 0.002$) and $\alpha_D^{-/-}$ ($P < 0.008$) mice compared with respective uninfected controls

lungs of animals with experimental MA-ARDS implies upregulation of $\alpha_D\beta_2$ and that $\alpha_D\beta_2$ on lung leukocytes has important activities in this condition. Of interest, $\alpha_D\beta_2$ is increased on the surfaces of leukocytes in the lungs of human subjects who died of ARDS triggered by other causes [51].

This study used mice with genetic deletion of α_D and consequent absence of $\alpha_D\beta_2$ [50] to examine its contributions to the pathophysiology of *P. berghei*-induced MA-ARDS. Specific blocking antibodies against the α_D subunit or $\alpha_D\beta_2$ are not commercially or generally available, making a genetic approach essential to target $\alpha_D\beta_2$ while leaving other leukocyte integrins intact [42, 44]. This study shows that key determinants of acute lung injury were improved in $\alpha_D^{-/-}$ animals at 7 days after infection. The seven-day time point was chosen because, in previous study of severe malaria caused by *P. berghei*, survival curves for wild type and $\alpha_D^{-/-}$ mice began to diverge at 7 days [50]. In the current experiments, lung leukocyte accumulation was reduced in $\alpha_D^{-/-}$ at 7 days. This finding is consistent with published evidence that $\alpha_D\beta_2$ mediates leukocyte accumulation and monocyte migration in tissue inflammation and injury in vivo [55, 57, 72], and that it mediates macrophage adhesion to tissue ligands [50] and purified protein targets [73] in vitro. In parallel, pulmonary vascular leak, evaluated by Evans Blue Dye extravasation [21, 62, 74], and increased permeability alveolar oedema, assayed by BALF protein concentration and lung weight [21, 62], were ameliorated in $\alpha_D\beta_2$-deficient animals. Thus, key determinants of the pathology and pathophysiology of acute alveolar injury in experimental and clinical ARDS [30, 62, 68] were improved in $\alpha_D^{-/-}$ animals in comparison to assessment of these variables in wild type mice. Furthermore, there was a similar pattern of improvement in airway function in $\alpha_D\beta_2$-deficient compared to wild type mice. AHR has not previously been examined in rodent models of malaria-induced pulmonary involvement. While airway hyperreactivity is not a prominent feature of ARDS triggered by sepsis and other common causes of ARDS [31, 68], cough, other symptoms of airway obstruction, and physiologic evidence for small airway narrowing and reactivity have been detected in patients with malaria [6, 7, 17, 19]. These findings suggest that airway dysfunction may contribute to the pathophysiology of MA-ARDS. Improvement in airway function in $\alpha_D^{-/-}$ mice indicates that airway inflammation is a mechanism of airway dysfunction in the *P. berghei* model. A trend in improvement was found in PV relationships in $\alpha_D^{-/-}$ mice, although this was not statistically significant.

Chemokine and cytokine levels were also reduced in the lungs of infected $\alpha_D^{-/-}$ mice compared to the levels in pulmonary tissue from wild type mice with MA-ARDS. This may be a key mechanism in improved alveolar inflammation, reduced alveolar-capillary leak, and reduction in alveolar oedema in $\alpha_D\beta_2$-deficient animals. Pro-inflammatory cytokines, including IL-1β, TNF, IL-8/KC, and others, are synthesized by alveolar macrophages and monocytes and are thought to drive alveolar inflammation and injury in experimental and clinical ARDS [30, 31, 68]. Cytokine imbalance is proposed to be a feature of the pathophysiology of clinical MA-ARDS [19]. In the studies reported here, intrapulmonary IL-1β, TNF, and KC were substantially reduced in infected $\alpha_D^{-/-}$ mice. Similarly, IL-12 and RANTES, which have pleiotropic activities in inflammation, were also reduced, as was MCP-1, which recruits monocytes to the lungs [75, 76]. Thus, reduced pro-inflammatory cytokines in infected $\alpha_D^{-/-}$ mice may in part account for reductions in the vascular and interstitial inflammation in these animals. Reductions in key cytokines may also account for improvement in alveolar-capillary barrier integrity and reduced leak of protein and fluid into the alveolar spaces of $\alpha_D\beta_2$-deficient mice compared to wild type mice with MA-ARDS. IL-1β and TNF are major agonists for endothelial VE cadherin internalization and endothelial barrier disruption in models of inflammatory injury, including experimental ARDS [77–79]. TNF and IL-1β were reduced to baseline levels in the lungs of infected $\alpha_D^{-/-}$ mice, potentially contributing to improved barrier function. Of note, a reduced systemic cytokine levels was also found in $\alpha_D\beta_2$-deficient mice infected with *P. berghei* in earlier analysis of this model [50]. The molecular events that mediate altered chemokine and cytokine levels in $\alpha_D\beta_2$-deficient mice are not yet completely defined. Nevertheless, in studies with human monocytes were found that engagement of $\alpha_D\beta_2$ with activating antibodies or specific ligands induces outside-in signaling to chemokine and cytokine synthetic pathways [51]. These evolving observations indicate that $\alpha_D\beta_2$, like other β_2 integrins [80, 81], is a key regulator of chemokine and cytokine gene expression in myeloid leukocytes.

Conversely, the release of cytokines, leads to cell activation and increased expression of adhesion molecules such as integrins and immunoglobulins superfamily members [82–84]. Several studies show the role of integrins in development pulmonary oedema, including beta integrins [85]. The main functions of CD11/CD18 integrins are adhesion and migration [86, 87], and previous studies showed that VCAM-1 is an important adhesion receptor in models of experimental [88] and human malaria [89–91] and is a potential ligand for leukocytes and PRBC, in cytoadherence processes that lead to obstruction of the microcirculation. This work demonstrate that the absence of CD11d integrin does not interfere in VCAM-1

expression, and suggest that the effects described in this work are due to an increased expression of CD11d integrin and not by a lack of its ligand. This study with VCAM-1 suggests increased endothelial activation during *P. berghei* infection, however, more experiments are necessary to better characterize this activation.

Conclusion

In conclusion, this report demonstrate that integrin $\alpha_D\beta_2$ is an important effector molecular in the inflammatory manifestations of severe *P. berghei* infection, including increased alveolar-capillary membrane permeability, alveolar monocyte and macrophage accumulation, and lung oedema, and that it is a key determinant of critical pathophysiologic events in this model of MA-ARDS. Blunting of acute lung injury in $\alpha_D\beta_2$-deficient mice likely contributes to the early survival advantage of $\alpha_D^{-/-}$ animals in lethal *P. berghei* infection, although they ultimately succumb to progressive hyperparasitaemia and severe malarial anaemia [50]. Other specific integrin heterodimers on a variety of cell types [41–43] may also contribute to the pathobiology of malarial infection, although this has been examined in only a limited fashion [92, 93]. Because of their diverse activities in inflammatory cell adhesion, accumulation, and signalling, $\alpha_D\beta_2$ and other leukocyte integrins may have pivotal roles in MA-ARDS, cerebral malaria and other complications of experimental and clinical malarial infection [44, 45, 71]. Dissection of the roles of leukocyte integrins will likely provide new insights into the innate and adaptive immune fabric of the host responses to Plasmodium, and increased understanding of cell- and organ-specific events in malarial inflammation.

Abbreviations

MA-ARDS: malaria-associated acute respiratory distress syndrome; ARDS: acute respiratory distress syndrome; RBC: red blood cell; BALF: bronchoalveolar lavage fluid; AHR: airway hyperreactivity; PV: lung pressure/volume; ETT: endotracheal tube; PMC: point of maximal compliance; PBS: phosphate buffer saline; HPRT: hypoxanthine guanine phosphoribosyl transferase.

Authors' contributions

IGAQ and AVA designed and performed the experiments, discussed the results, analysed the data, and wrote the manuscript. ACF, DON, AMS, TPTF, TMG, and GMR designed and performed the experiments, discussed the results and analysed the data. RAC and ARC discussed the results and analysed the data. IGAQ, AVA, GAZ, and HCCFN conceived and designed the study, discussed the results and wrote the manuscript. PTB, PMRS and GAZ reviewed the manuscript. AVA, PMRS, PTB, GAZ, and HCCFN funded this work. All authors read and approved the final manuscript.

Author details

[1] Laboratório de Immunofarmacologia, Instituto Oswaldo Cruz, Fiocruz, Pavilhão Ozório de Almeida, Av. Brasil 4365, Manguinhos, Rio de Janeiro, RJ CEP 21045-900, Brazil. [2] Program in Molecular Medicine, Department of Internal Medicine, University of Utah, Salt Lake City, UT, USA. [3] Laboratório de Inflamação, Instituto Oswaldo Cruz, Fiocruz, Pavilhão Ozório de Almeida, Rio de Janeiro, Brazil. [4] Laboratório de Engenharia Pulmonar no Programa de Engenharia Biomédica, Instituto Alberto Luiz Coimbra de Pós-Graduação e Pesquisa de Engenharia-COPPE/Universidade Federal do Rio de Janeiro, Rio de Janeiro, Brazil. [5] Laboratório de Fisiologia da Respiração, Instituto de Biofísica Carlos Chagas Filho, Universidade Federal do Rio de Janeiro, Rio de Janeiro, Brazil. [6] Programa de Produtividade Científica, Universidade Estácio de Sá, Rio de Janeiro, RJ, Brazil.

Acknowledgements

The authors are grateful to Dr. Leonardo Carvalho for kindly providing the *P. berghei* ANKA strain and Dr. Patricia Alves Reis for all assistance during work.

Competing interests

The authors declare that they have no competing interests.

Ethics approval and consent to participate

All animal experimental procedures used in this study were approved by the Committee of ethical animal use Oswaldo Cruz Foundation, under license number L-033/09.

Funding

This work was supported by the Conselho de Desenvolvimento Científico e Tecnológico (CNPq), Fundação de Amparo a Pesquisa do Estado do Rio de Janeiro (FAPERJ), PROEP-IOC, Programa de Núcleos de Excelência (Pronex) of the government of Brazil and a grant from the U.S. National Institutes of Health (MERIT Award R37HL044525 to GAZ). GAZ is the recipient of a Ciencia Sem Fronteiras (Science Without Borders) Special Visiting Professorship from CNPq.

Received: 19 September 2015 Accepted: 20 July 2016
Published online: 30 July 2016

References

1. WHO. World malaria report 2015. Geneva: World Health Organization; 2015. p. 8–21.
2. Stevenson MM, Riley EM. Innate immunity to malaria. Nat Rev Immunol. 2004;4:169–80.
3. White NJ, Pukrittayakamee S, Hien TT, Faiz MA, Mokuolu OA, Dondorp AM. Malaria. Lancet. 2014;383:723–35.
4. Taylor BM, Kolbasa KP, Chin JE, Richards IM, Fleming WE, Griffin RL, et al. Roles of adhesion molecules ICAM-1 and α4 integrin in antigen-induced changes in microvascular permeability associated with lung inflammation in sensitized brown Norway rats. Am J Respir Cell Mol Biol. 1997;17:757–66.
5. Schofield L, Grau GE. Immunological processes in malaria pathogenesis. Nat Rev Immunol. 2005;5:722–35.
6. Anstey NM, Jacups SP, Cain T, Pearson T, Ziesing PJ, Fisher DA, et al. Pulmonary manifestations of uncomplicated falciparum and vivax malaria: cough, small airways obstruction, impaired gas transfer, and increased pulmonary phagocytic activity. J Infect Dis. 2002;185:1326–34.
7. Taylor WR, Canon V, White NJ. Pulmonary manifestations of malaria: recognition and management. Treat Respir Med. 2006;5:419–28.
8. Taylor WR, White NJ. Malaria and the lung. Clin Chest Med. 2002;23:457–68.
9. Jindal SK, Aggarwal AN, Gupta D. Adult respiratory distress syndrome in the tropics. Clin Chest Med. 2002;23:445–55.
10. Lee EY, Maguire JH. Acute pulmonary edema complicating ovale malaria. Clin Infect Dis. 1999;29:697–8.
11. Haydoura S, Mazboudi O, Charafeddine K, Bouakl I, Baban TA, Taher AT, Kanj SS. Transfusion-related *Plasmodium ovale* malaria complicated by acute respiratory distress syndrome (ARDS) in a non-endemic country. Parasitol Int. 2010;60:114–6.
12. Price L, Planche T, Rayner C, Krishna S. Acute respiratory distress syndrome in *Plasmodium vivax* malaria: case report and review of the literature. Trans R Soc Trop Med Hyg. 2007;101:655–9.
13. Sarkar S, Saha K, Das CS. Three cases of ARDS: an emerging complication of *Plasmodium vivax* malaria. Lung India. 2010;27:154–7.
14. Kumar S, Melzer M, Dodds P, Watson J, Ord RP. *vivax* malaria complicated by shock and ARDS. Scand J Infect Dis. 2007;39:255–6.

15. Lomar AV, Vidal JE, Lomar FP, Barbas CV, de Matos GJ, Boulos M. Acute respiratory distress syndrome due to vivax malaria: case report and literature review. Braz J Infect Dis. 2005;9:425–30.
16. Agarwal R, Nath A, Gupta D. Noninvasive ventilation in *Plasmodium vivax* related ALI/ARDS. Intern Med. 2007;46:2007–11.
17. Maguire GP, Handojo T, Pain MC, Kenangalem E, Price RN, Tjitra E, et al. Lung injury in uncomplicated and severe falciparum malaria: a longitudinal study in Papua, Indonesia. J Infect Dis. 2005;192:1966–74.
18. Mohan A, Sharma SK, Bollineni S. Acute lung injury and acute respiratory distress syndrome in malaria. J Vector Borne Dis. 2008;45:179–93.
19. Taylor WR, Hanson J, Turner GD, White NJ, Dondorp AM. Respiratory manifestations of malaria. Chest. 2012;142:492–505.
20. Barber BE, William T, Grigg MJ, Menon J, Auburn S, Marfurt J, et al. A prospective comparative study of knowlesi, falciparum, and vivax malaria in Sabah, Malaysia: high proportion with severe disease from *Plasmodium knowlesi* and *Plasmodium vivax* but no mortality with early referral and artesunate therapy. Clin Infect Dis. 2013;56:383–97.
21. Van den Steen PE, Deroost K, Deckers J, Van Herck E, Struyf S, Opdenakker G. Pathogenesis of malaria-associated acute respiratory distress syndrome. Trends Parasitol. 2013;29:346–58.
22. Trampuz A, Jereb M, Muzlovic I, Prabhu RM. Clinical review. Severe malaria. Crit Care. 2003;7:315–23.
23. Charoenpan P, Indraprasit S, Kiatboonsri S, Suvachittanont O, Tanomsup S. Pulmonary edema in severe falciparum malaria. Hemodynamic study and clinicophysiologic correlation. Chest. 1990;97:1190–7.
24. Brooks MH, Kiel FW, Sheehy TW, Barry KG. Acute pulmonary edema in falciparum malaria—a clinicopathological correlation. N Engl J Med. 1968;279:732–7.
25. Rogerson SJ, Grau GE, Hunt NH. The microcirculation in severe malaria. Microcirculation. 2004;11:559–76.
26. Anstey NM, Handojo T, Pain MC, Kenangalem E, Tjitra E, Price RN, et al. Lung injury in vivax malaria: pathophysiological evidence for pulmonary vascular sequestration and posttreatment alveolar-capillary inflammation. J Infect Dis. 2007;195:589–96.
27. Anstey NM, Russell B, Yeo TW, Price RN. The pathophysiology of vivax malaria. Trends Parasitol. 2009;25:220–7.
28. Valecha N, Pinto RG, Turner GD, Kumar A, Rodrigues S, Dubhashi NG, Rodrigues E, et al. Histopathology of fatal respiratory distress caused by *Plasmodium vivax* malaria. Am J Trop Med Hyg. 2009;81:758–62.
29. Lacerda MV, Fragoso SC, Alecrim MG, Alexandre MA, Magalhaes BM, Siqueira AM, et al. Postmortem characterization of patients with clinical diagnosis of *Plasmodium vivax* malaria: to what extent does this parasite kill? Clin Infect Dis. 2012;55:67–74.
30. Matthay MA, Ware LB, Zimmerman GA. The acute respiratory distress syndrome. J Clin Invest. 2012;122:2731–40.
31. Matthay MA, Zemans RL. The acute respiratory distress syndrome: pathogenesis and treatment. Annu Rev Pathol. 2011;6:147–63.
32. Pettersson F, Vogt AM, Jonsson C, Mok BW, Shamaei-Tousi A, Bergstrom S, et al. Whole-body imaging of sequestration of *Plasmodium falciparum* in the rat. Infect Immun. 2005;73:7736–46.
33. Lovegrove FE, Gharib SA, Pena-Castillo L, Patel SN, Ruzinski JT, Hughes TR, et al. Parasite burden and CD36-mediated sequestration are determinants of acute lung injury in an experimental malaria model. PLoS Pathog. 2008;4:e1000068.
34. Epiphanio S, Campos MG, Pamplona A, Carapau D, Pena AC, Ataide R, et al. VEGF promotes malaria-associated acute lung injury in mice. PLoS Pathog. 2010;6:e1000916.
35. Van den Steen PE, Geurts N, Deroost K, Van Aelst I, Verhenne S, Heremans H, et al. Immunopathology and dexamethasone therapy in a new model for malaria-associated acute respiratory distress syndrome. Am J Respir Crit Care Med. 2010;181:957–68.
36. Hee L, Dinudom A, Mitchell AJ, Grau GE, Cook DI, Hunt NH, et al. Reduced activity of the epithelial sodium channel in malaria-induced pulmonary oedema in mice. Int J Parasitol. 2011;41:81–8.
37. Deroost K, Tyberghein A, Lays N, Noppen S, Schwarzer E, Vanstreels E, et al. Hemozoin induces lung inflammation and correlates with malaria-associated acute respiratory distress syndrome. Am J Respir Cell Mol Biol. 2013;48:589–600.
38. Ortolan LS, Sercundes MK, Barboza R, Debone D, Murillo O, Hagen SC, et al. Predictive criteria to study the pathogenesis of malaria-associated ALI/ARDS in mice. Mediators Inflamm. 2014;2014:872464.
39. Franke-Fayard B, Janse CJ, Cunha-Rodrigues M, Ramesar J, Buscher P, Que I, et al. Murine malaria parasite sequestration: CD36 is the major receptor, but cerebral pathology is unlinked to sequestration. Proc Natl Acad Sci USA. 2005;102:11468–73.
40. White NJ, Turner GD, Medana IM, Dondorp AM, Day NP. The murine cerebral malaria phenomenon. Trends Parasitol. 2010;26:11–5.
41. Barczyk M, Carracedo S, Gullberg D. Integrins. Cell Tissue Res. 2010;339:269–80.
42. Lowell CA, Mayadas TN. Overview: studying integrins in vivo. Methods Mol Biol. 2012;757:369–97.
43. Hynes RO. Integrins: bidirectional, allosteric signaling machines. Cell. 2002;110:673–87.
44. Harris ES, Weyrich AS, Zimmerman GA. Lessons from rare maladies: leukocyte adhesion deficiency syndromes. Curr Opin Hematol. 2013;20:16–25.
45. Evans R, Patzak I, Svensson L, De Filippo K, Jones K, McDowall A, et al. Integrins in immunity. J Cell Sci. 2009;122:215–25.
46. Yonekawa K, Harlan JM. Targeting leukocyte integrins in human diseases. J Leukoc Biol. 2005;77:129–40.
47. Danilenko DM, Rossitto PV, Van der Vieren M, Le Trong H, McDonough SP, Affolter VK, et al. A novel canine leukointegrin, $\alpha_b\beta_2$, is expressed by specific macrophage subpopulations in tissue and a minor CD8+ lymphocyte subpopulation in peripheral blood. J Immunol. 1995;155:35–44.
48. Van der Vieren M, Le Trong H, Wood CL, Moore PF, St John T, Staunton DE, et al. A novel leukointegrin, $\alpha_b\beta_2$, binds preferentially to ICAM-3. Immunity. 1995;3:683–90.
49. Wu H, Rodgers JR, Perrard XY, Perrard JL, Prince JE, Abe Y, et al. Deficiency of CD11b or CD11d results in reduced staphylococcal enterotoxin-induced T cell response and T cell phenotypic changes. J Immunol. 2004;173:297–306.
50. Miyazaki Y, Bunting M, Stafforini DM, Harris ES, McIntyre TM, Prescott SM, et al. Integrin $\alpha_D\beta_2$ is dynamically expressed by inflamed macrophages and alters the natural history of lethal systemic infections. J Immunol. 2008;180:590.
51. Miyazaki Y, Vieira-de-Abreu A, Harris ES, Shah AM, Weyrich AS, Castro-Faria-Neto HC, et al. Integrin $\alpha_D\beta_2$ (CD11d/CD18) is expressed by human circulating and tissue myeloid leukocytes and mediates inflammatory signaling. PLoS One. 2014;9:e112770.
52. El-Gabalawy H, Canvin J, Ma GM, Van der Vieren M, Hoffman P, Gallatin M, et al. Synovial distribution of α_b/CD18, a novel leukointegrin. Comparison with other integrins and their ligands. Arthritis Rheum. 1996;39:1913–21.
53. Shanley TP, Warner RL, Crouch LD, Dietsch GN, Clark DL, O'Brien MM, et al. Requirements for α_b in IgG immune complex-induced rat lung injury. J Immunol. 1998;160:1014–20.
54. Yakubenko VP, Belevych N, Mishchuk D, Schurin A, Lam SC, Ugarova TP. The role of integrin $\alpha_D\beta_2$ (CD11d/CD18) in monocyte/macrophage migration. Exp Cell Res. 2008;314:2569–78.
55. Saville LR, Pospisil CH, Mawhinney LA, Bao F, Simedrea FC, Peters AA, et al. A monoclonal antibody to CD11d reduces the inflammatory infiltrate into the injured spinal cord: a potential neuroprotective treatment. J Neuroimmunol. 2004;156:42–57.
56. Bao F, Dekaban GA, Weaver LC. Anti-CD11d antibody treatment reduces free radical formation and cell death in the injured spinal cord of rats. J Neurochem. 2005;94:1361–73.
57. Utagawa A, Bramlett HM, Daniels L, Lotocki G, Dekaban GA, Weaver LC, Dietrich WD. Transient blockage of the CD11d/CD18 integrin reduces contusion volume and macrophage infiltration after traumatic brain injury in rats. Brain Res. 2008;1207:155–63.
58. Reis PA, Comim CM, Hermani F, Silva B, Barichello T, Portella AC, et al. Cognitive dysfunction is sustained after rescue therapy in experimental cerebral malaria, and is reduced by additive antioxidant therapy. PLoS Pathog. 2010;6:e1000963.
59. Thumwood CM, Hunt NH, Clark IA, Cowden WB. Breakdown of the blood-brain barrier in murine cerebral malaria. Parasitology. 1988;96:579–89.
60. Abreu SC, Antunes MA, Maron-Gutierrez T, Cruz FF, Ornellas DS, Silva AL, et al. Bone marrow mononuclear cell therapy in experimental allergic asthma: intratracheal versus intravenous administration. Respir Physiol Neurobiol. 2013;185:615–24.
61. Hoebe K, Georgel P, Rutschmann S, Du X, Mudd S, Crozat K, et al. CD36 is a sensor of diacylglycerides. Nature. 2005;433:523–7.

62. Matute-Bello G, Downey G, Moore BB, Groshong SD, Matthay MA, Slutsky AS, et al. An official American Thoracic Society workshop report: features and measurements of experimental acute lung injury in animals. Am J Respir Cell Mol Biol. 2011;44:725–38.
63. Gordon S, Taylor PR. Monocyte and macrophage heterogeneity. Nat Rev Immunol. 2005;5:953–64.
64. Wynn TA, Chawla A, Pollard JW. Macrophage biology in development, homeostasis and disease. Nature. 2013;496:445–55.
65. Grayson MH, Van der Vieren M, Sterbinsky SA, Gallatin WM, Hoffman PA, Staunton DE, Bochner BS. $\alpha_D\beta_2$ integrin is expressed on human eosinophils and functions as an alternative ligand for vascular cell adhesion molecule 1 (VCAM-1). J Exp Med. 1998;188:2187–91.
66. Van der Vieren M, Crowe DT, Hoekstra D, Vazeux R, Hoffman PA, Grayson MH, et al. The leukocyte integrin $\alpha_D\beta_2$ binds VCAM-1: evidence for a binding interface between I domain and VCAM-1. J Immunol. 1999;163:1984–90.
67. Albertine KH, Wang L, Watanabe S, Marathe GK, Zimmerman GA, McIntyre TM. Temporal correlation of measurements of airway hyperresponsiveness in ovalbumin-sensitized mice. Am J Physiol Lung Cell Mol Physiol. 2002;283:219–33.
68. Ware LB. Pathophysiology of acute lung injury and the acute respiratory distress syndrome. Semin Respir Crit Care Med. 2006;27:337–49.
69. Schofield L. Intravascular infiltrates and organ-specific inflammation in malaria pathogenesis. Immunol Cell Biol. 2007;85:130–7.
70. Gillrie MR, Krishnegowda G, Lee K, Buret AG, Robbins SM, Looareesuwan S, et al. Src-family kinase dependent disruption of endothelial barrier function by *Plasmodium falciparum* merozoite proteins. Blood. 2007;110:3426–35.
71. Lee SH, Corry DB. Homing alone? CD18 in infectious and allergic disease. Trends Mol Med. 2004;10:258–62.
72. Mabon PJ, Weaver LC, Dekaban GA. Inhibition of monocyte/macrophage migration to a spinal cord injury site by an antibody to the integrin α_D: a potential new anti-inflammatory treatment. Exp Neurol. 2000;166:52–64.
73. Yakubenko VP, Yadav SP, Ugarova TP. Integrin $\alpha_D\beta_2$, an adhesion receptor up-regulated on macrophage foam cells, exhibits multiligand-binding properties. Blood. 2006;107:1643–50.
74. van der Heyde HC, Bauer P, Sun G, Chang WL, Yin L, Fuseler J, et al. Assessing vascular permeability during experimental cerebral malaria by a radiolabeled monoclonal antibody technique. Infect Immun. 2001;69:3460–5.
75. Huffnagle GB, Strieter RM, Standiford TJ, McDonald RA, Burdick MD, Kunkel SL, et al. The role of monocyte chemotactic protein-1 (MCP-1) in the recruitment of monocytes and CD4 + T cells during a pulmonary *Cryptococcus neoformans* infection. J Immunol. 1995;155:4790–7.
76. Gunn MD, Nelken NA, Liao X, Williams LT. Monocyte chemoattractant protein-1 is sufficient for the chemotaxis of monocytes and lymphocytes in transgenic mice but requires an additional stimulus for inflammatory activation. J Immunol. 1997;158:376–83.
77. Pober JS, Sessa WC. Evolving functions of endothelial cells in inflammation. Nat Rev Immunol. 2007;7:803–15.
78. London NR, Zhu W, Bozza FA, Smith MC, Greif DM, Sorensen LK, et al. Targeting Robo4-dependent Slit signaling to survive the cytokine storm in sepsis and influenza. Sci Transl Med. 2010;2:23ra19.
79. Zhu W, London NR, Gibson CC, Davis CT, Tong Z, Sorensen LK, et al. Interleukin receptor activates a MYD88-ARNO-ARF6 cascade to disrupt vascular stability. Nature. 2012;492:252–5.
80. Walzog B, Weinmann P, Jeblonski F, Scharffetter-Kochanek K, Bommert K, Gaehtgens P. A role for β(2) integrins (CD11/CD18) in the regulation of cytokine gene expression of polymorphonuclear neutrophils during the inflammatory response. Faseb J. 1999;13:1855–65.
81. Rezzonico R, Imbert V, Chicheportiche R, Dayer JM. Ligation of CD11b and CD11c β(2) integrins by antibodies or soluble CD23 induces macrophage inflammatory protein 1α (MIP-1α) and MIP-1β production in primary human monocytes through a pathway dependent on nuclear factor-κB. Blood. 2001;97:2932–40.
82. Vanderstocken G, Bondue B, Horckmans M, Di Pietrantonio L, Robaye B, Boeynaems JM, Communi D. P2Y2 receptor regulates VCAM-1 membrane and soluble forms and eosinophil accumulation during lung inflammation. J Immunol. 2010;185:3702–7.
83. Li ZP, Hu JF, Sun MN, Ji HJ, Chu SF, Liu G, Chen NH. Anti-inflammatory effect of IMMLG5521, a coumarin derivative, on sephadex-induced lung inflammation in rats. Int Immunopharmacol. 2012;14(2):145–9.
84. Silva AC, Vieira RP, Nisiyama M, Santos AB, Perini A, Mauad T, et al. Exercise inhibits allergic lung inflammation. Int J Sports Med. 2012;33:402–9.
85. Reiss LK, Uhlig U, Uhlig S. Models and mechanisms of acute lung injury caused by direct insults. Eur J Cell Biol. 2012;91:590–601.
86. Harris ES, McIntyre TM, Prescott SM, Zimmerman GA. The leukocyte integrins. J Biol Chem. 2000;275:23409–12.
87. Golias C, Batistatou A, Bablekos G, Charalabopoulos A, Peschos D, Mitsopoulos P, et al. Physiology and pathophysiology of selectins, integrins, and IgSf cell adhesion molecules focusing on inflammation. A paradigm model on infectious endocarditis. Cell Commun Adhes. 2011;18:19–32.
88. Zanini GM, Cabrales P, Barkho W, Frangos JA, Carvalho LJ. Exogenous nitric oxide decreases brain vascular inflammation, leakage and venular resistance during *Plasmodium berghei* ANKA infection in mice. J Neuroinflammation. 2011;8:66.
89. Fatih FA, Siner A, Ahmed A, Woon LC, Craig AG, Singh B, et al. Cytoadherence and virulence—the case of *Plasmodium knowlesi* malaria. Malar J. 2012;11:33.
90. Wu Y, Szestak T, Stins M, Craig AG. Amplification of *P. falciparum* cytoadherence through induction of a pro-adhesive state in host endothelium. PLoS One. 2011;6:e24784.
91. Janes JH, Wang CP, Levin-Edens E, Vigan-Womas I, Guillotte M, Melcher M, et al. Investigating the host binding signature on the *Plasmodium falciparum* PfEMP1 protein family. PLoS Pathog. 2011;7:e1002032.
92. Senaldi G, Vesin C, Chang R, Grau GE, Piguet PF. Role of polymorphonuclear neutrophil leukocytes and their integrin CD11a (LFA-1) in the pathogenesis of severe murine malaria. Infect Immun. 1994;62:1144–9.
93. van der Heyde HC, Gramaglia I, Sun G, Woods C. Platelet depletion by anti-CD41 (αIIb) mAb injection early but not late in the course of disease protects against *Plasmodium berghei* pathogenesis by altering the levels of pathogenic cytokines. Blood. 2005;105:1956–63.